Shell-model study for neutron-rich *sd*-shell nuclei

Kazunari Kaneko,[1] Yang Sun,[2,3] Takahiro Mizusaki,[4] and Munetake Hasegawa[2]
[1]*Department of Physics, Kyushu Sangyo University, Fukuoka 813-8503, Japan*
[2]*Institute of Modern Physics, Chinese Academy of Sciences, Lanzhou 730000, People's Republic of China*
[3]*Department of Physics, Shanghai Jiao Tong University, Shanghai 200240, People's Republic of China*
[4]*Institute of Natural Sciences, Senshu University, Tokyo 101-8425, Japan*
(Received 4 August 2010; revised manuscript received 3 December 2010; published 31 January 2011)

The microscopic structure of neutron-rich *sd*-shell nuclei is investigated by using the spherical-shell model in the *sd*-*pf* valence space with the extended pairing plus quadrupole-quadrupole forces accompanied by the monopole interaction (EPQQM). The calculation reproduces systematically the known energy levels for even-even and odd-mass nuclei including the recent data for ^{43}S, ^{46}S, and ^{47}Ar. In particular, the erosion of the $N = 28$ shell closure in ^{42}Si can be explained. Our EPQQM results are compared with other shell-model calculations with the SDPF-NR and SDPF-U effective interactions.

DOI: 10.1103/PhysRevC.83.014320 PACS number(s): 21.10.Dr, 21.60.Cs, 21.10.Re, 27.40.+z

I. INTRODUCTION

The current experimental and theoretical investigation focuses on the study of evolution of nuclear structure around the shell gap at $N = 28$. The $N = 28$ shell closure is a traditional one in the nuclear single-particle spectrum driven by the spin-orbit interaction. For example, the ^{48}Ca nucleus has been known to exhibit double magicity as a result of the neutron subshell gap separating the $f_{7/2}$ orbit and the $f_{5/2}p$ shells at $N = 28$. However, recent theoretical studies and experimental data have questioned the persistence of the traditional magic numbers and revealed that the $N = 28$ shell gap is eroded when moving away from the stability line. The experimental data for the ^{44}S and ^{42}Si isotones indicate a clear breaking of the $N = 28$ magicity because of the observed small 2^+ energy [1–3]. Recently, direct evidence of collapse of the $N = 28$ shell closure due to the level inversion between the lowest $7/2^-$ and $3/2^-$ levels has been observed in ^{43}S [4]. In addition, toward $N = 28$, the degeneracy between the lowest $1/2^+$ and $3/2^+$ states in the odd-proton P, Cl, and K isotopes suggests [5] that the shell gap between the $d_{3/2}$ and $s_{1/2}$ proton orbits almost collapses at $N = 28$. The reduction of the $N = 28$ neutron gap combined with this degeneracy is regarded as the possible origin of erosion of the $N = 28$ magicity in the neutron-rich *sd*-shell nuclei.

To gain the insight into the evolution of shell structure in the neutron-rich *sd*-shell nuclei and to understand the details of collapse of the $N = 28$ magicity, shell-model calculations in the full *sd*-*pf* space are desirable. However, conventional shell-model calculations in the full *sd*-*pf* space are not possible at present because of the huge dimension in the configuration space. To study the neutron-rich *sd*-shell nuclei, therefore, one needs to incorporate truncations in the valence space. One choice is such that valence protons are restricted to the *sd* shell and neutrons to the *sd*-*pf* shell with twelve *sd* frozen neutrons. Such an approach was originally introduced with the effective interaction SDPF-NR [6–10]. The nuclei in this mass region are known to have a variety of shapes (e.g., shape coexistence discussed in Refs. [2,4]), and the nucleus ^{42}Si has been the subject of debate on its magic nature [3,11]. The SDPF-NR interaction was applied to the neutron-rich *sd*-shell nuclei, and one found that it describes well the excitation energies for very neutron-rich isotopes with $Z > 14$. However, the calculation deviated from the experimental data for the silicon ($Z = 14$) isotopes where the calculated energies for $^{36-42}$Si were too high. To improve the results, the *pf*-shell effective interaction in SDPF-NR was renormalized to compensate for the absence of $2p$-$2h$ excitations from the core [12]. With the reduction of pairing in the renormalization for $Z \leqslant 14$, the 2_1^+ excitation energies in silicon isotopes agreed nicely with experimental results. Thus, two SDPF-U interactions, one for $Z > 14$ and the other for $Z \leqslant 14$, are respectively needed for the description of collectivity at $N = 28$ in the isotopic chains of sulfur ($Z = 16$) and silicon ($Z = 14$). In a similar way, the SDPF-NR2 and SDPF-NR3 interactions have recently been suggested to describe the sudden change in nuclear structure at $N = 28$ [13]. From this discussion, one sees that a consistent shell-model treatment for collectivity at the $N = 28$ shell closure in different isotopic chains has not been successful so far.

The main purpose of the present article is to construct a unified effective interaction for the neutron-rich *sd*-shell nuclei, which can be consistently applicable to both $Z > 14$ and $Z \leqslant 14$ isotopic chains, and to understand the shell evolution in this exotic mass region. It is well known that realistic effective interactions used in the low-energy nuclear structure study are dominated by the pairing plus quadrupole-quadrupole ($P + QQ$) forces with inclusion of the monopole term [14]. As documented in the literature, the extended $P + QQ$ model combined with the monopole interaction works well for a wide range of nuclei [15,16]. This effective interaction is called hereafter EPQQM to distinguish it from shell models with other effective interactions. The EPQQM model has demonstrated its capability of describing the microscopic structure in different $N \approx Z$ nuclei, as for instance, in the *fp*-shell region [15] and the *fpg*-shell region [16]. Recently, it has been shown that the EPQQM model is also applicable to the neutron-rich Cr isotopes [17].

The monopole interaction plays an important role in our discussion. The monopole shifts in the spherical-shell model have been introduced to account for the nonconventional

shell evolution in neutron-rich nuclei. Connection between the monopole shifts and the tensor force [18] has been studied within the self-consistent mean-field model using the Gogny force [19]. It has recently been clarified that the possible physical origin of these interactions is attributed to the central and tensor forces [20,21]. For example, when one goes from the Ca down to the Si isotopes, a significant reduction of the $N = 28$ shell gap can be found. By removing protons from the $d_{3/2}$ orbit in nuclei between Ca and Si, the strong attractive proton-neutron monopole force between the $\pi d_{3/2}$ and $\nu f_{7/2}$ orbits is no longer present [12,22]. This makes the neutron $f_{7/2}$ less bound and thus reduces the size of the $N = 28$ gap in nuclei between ^{40}Ca and ^{34}Si.

The paper is arranged as follows. In Sec. II, we outline our model. In Sec. III, we perform the numerical calculations and discuss the results for the neutron-rich nuclei in the sd-pf shell region. Finally, conclusions are drawn in Sec. IV.

II. THE MODEL

We start with the following form of Hamiltonian, which consists of pairing and quadrupole-quadrupole terms with the monopole interaction

$$\begin{aligned} H &= H_{\rm sp} + H_{P_0} + H_{P_2} + H_{QQ} + H_{\rm m} \\ &= \sum_{\alpha} \varepsilon_a c^{\dagger}_{\alpha} c_{\alpha} - \sum_{J=0,2} \frac{1}{2} g_J \sum_{M\kappa} P^{\dagger}_{JM1\kappa} P_{JM1\kappa} \\ &\quad - \frac{1}{2} \chi_2 / b^4 \sum_{M} : Q^{\dagger}_{2M} Q_{2M} : \\ &\quad + \sum_{a \leqslant b} \sum_{T} k^{T}_{\rm m}(ab) \sum_{JMK} A^{\dagger}_{JMTK}(ab) A_{JMTK}(ab), \end{aligned} \quad (1)$$

where b in the third term is the length parameter of harmonic oscillator. We take the $J = 0$ and $J = 2$ forces in the pairing channel, and the quadrupole-quadrupole (QQ) forces in the particle-hole channel [15,16]. The monopole interaction is denoted by $H_{\rm m}$, where the global monopole force is neglected because it does not affect the excitation energies of the low-lying states. This isospin-invariant Hamiltonian (1) is diagonalized in a chosen model space based on the spherical basis. We employ the shell-model code ANTOINE [23] for the numerical calculation. In the present work, we consider an ^{16}O core and employ the sd-pf model space comprising the $0d_{5/2}$, $1s_{1/2}$, and $0d_{3/2}$ active proton orbitals and the $0d_{5/2}$, $1s_{1/2}$, $0d_{3/2}$, $0f_{7/2}$, $1p_{3/2}$, and $0f_{5/2}$, $1p_{1/2}$ active neutron orbitals with twelve sd frozen neutrons. We employ the same single-particle energies as those of Ref. [12]: $\varepsilon_{d5/2} = 0.0$, $\varepsilon_{s1/2} = 0.78$, $\varepsilon_{d3/2} = 5.60$, $\varepsilon_{f7/2} = 9.92$, $\varepsilon_{p3/2} = 10.01$, $\varepsilon_{p1/2} = 15.15$, and $\varepsilon_{f5/2} = 10.18$ (all in MeV). We adopt the following interaction strengths for the EPQQM forces: $g_0 = 0.540$, $g_2 = 0.678$, and $\chi_2 = 0.474$ (all in MeV). Finally, for the monopole terms, the strengths are chosen to be (all in MeV)

$$\begin{aligned} &k^{T=0}_{\rm m}(f_{7/2}, d_{3/2}) = -0.65, \quad k^{T=0}_{\rm m}(f_{7/2}, d_{5/2}) = -0.3, \\ &k^{T=0}_{\rm m}(d_{5/2}, p_{1/2}) = 0.55, \quad k^{T=0}_{\rm m}(d_{5/2}, p_{3/2}) = -0.2, \\ &k^{T=0}_{\rm m}(d_{3/2}, p_{3/2}) = 0.5, \quad k^{T=0}_{\rm m}(s_{1/2}, p_{3/2}) = -0.6, \end{aligned} \quad (2)$$

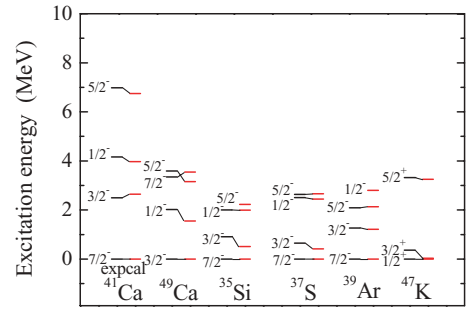

FIG. 1. (Color online) Comparison of experimental and calculated energy levels for the odd-mass nuclei near the neutron or proton shell closure in the sd region. The left (black) and right (red) bars denote the experimental and calculated energy levels, respectively.

$$\begin{aligned} &k^{T=1}_{\rm m}(d_{5/2}, d_{3/2}) = -0.2, \quad k^{T=1}_{\rm m}(f_{7/2}, f_{5/2}) = -0.1, \\ &k^{T=1}_{\rm m}(f_{7/2}, p_{1/2}) = -0.01, \quad k^{T=1}_{\rm m}(f_{7/2}, p_{3/2}) = -0.03, \\ &k^{T=1}_{\rm m}(f_{7/2}, f_{7/2}) = -0.3, \quad k^{T=1}_{\rm m}(p_{3/2}, p_{3/2}) = -0.45. \end{aligned}$$

The rest of the monopole terms are neglected in the present calculations. The previous EPQQM force strengths are determined so as to reproduce the experimental energy levels for odd-mass nuclei that have one particle or one hole on top of the neutron and proton shell closures. The results are compared with experimental data [24] in Fig. 1. Here the root mean square (rms) deviations between the experimental and theoretical excitation energies are 0.24, 0.14, and 0.20 (in MeV) for the $3/2^-$, $1/2^-$, and $5/2^-$ states, respectively, which means that the agreement is good. We emphasize that in order to describe the data correctly, a very important part of the interaction is those monopole forces. It has recently been proposed that the attractive $T = 0$ monopole interactions $\pi d_{3/2}$-$\nu f_{7/2}$ and $\pi d_{5/2}$-$\nu f_{7/2}$ be attributed to the monopole effect of the central and tensor forces in the nucleon-nucleon interaction [20,21], where the central term produces a global contribution and the tensor term generates local variations. They are responsible for the collapse of the $N = 28$ shell closure in the neutron-rich sd-shell nuclei, which gives rise to the drastic change in nuclear shape of the $N = 28$ isotones. In fact, it has been reported that the tensor force produces the pronounced oblate minimum in the potential energy surface for ^{42}Si [22]. Along the K isotopic chains, the repulsive $\pi d_{3/2}$-$\nu p_{3/2}$ and attractive $\pi s_{1/2}$-$\nu p_{3/2}$ monopole interactions lead to an inversion of the expected ordering in the lowest $3/2^+$ and $1/2^+$ levels in ^{47}K. In addition, these interactions reproduce the evolution of the lowest $3/2^-$ state in ^{35}Si. The monopole interactions between $\pi d_{5/2}$ and the pf shells act so as to reproduce the low-lying states in ^{49}Ca.

III. NUMERICAL RESULTS AND DISCUSSION

A. The shell erosion in $N = 28$

We discuss changes in the shell structure when moving away from the valley of stability. Large energy gaps at the traditional magic numbers in stable nuclei may be washed out in the neutron- or proton-rich regions. The fundamental question of how the nuclear-shell structure evolves with proton or neutron excess is one of the main motivations to study nuclei

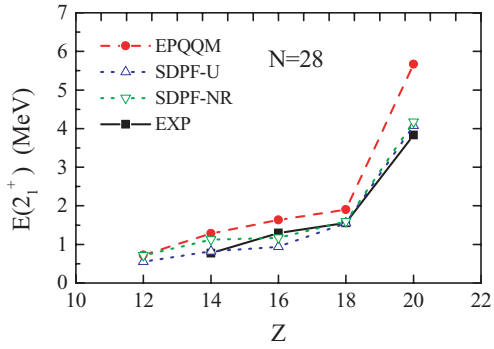

FIG. 2. (Color online) Experimental and calculated first excited 2^+ energies $E(2_1^+)$ for the neutron-rich $N = 28$ isotones.

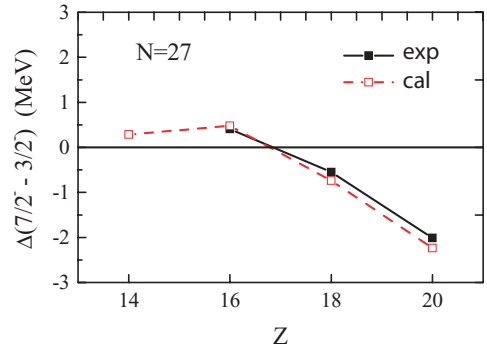

FIG. 4. (Color online) Energy splitting between the lowest $7/2^-$ and $3/2^-$ states in neutron-rich $N = 27$ isotones [4,25,26].

far from stability. The study of shapes in such exotic nuclei serves as a sensitive test for the predictive power of nuclear models. Figure 2 shows the systematics of the first excited 2^+ states for the $N = 28$ isotones, which are compared with three shell-model calculations with the EPQQM, SDPF-U, and SDPF-NR effective interactions. As one can see, all the calculations are capable of producing the drastic drop in energy when removing protons from the double magic nucleus ^{48}Ca.

To understand the erosion of the $N = 28$ shell gap, the neutron effective single-particle energies (ESPE) as a function of proton number are shown in Fig. 3. The $\nu f_{7/2}$ and $\nu p_{3/2}$ orbitals at $Z = 20$ become degenerate at $Z = 16$. This degeneracy is due to the attractive proton-neutron monopole interaction between the $\nu f_{7/2}$ and $\pi d_{3/2}$ orbitals. As seen in Fig. 4, the inversion of the lowest $7/2^-$ and $3/2^-$ states in ^{43}S ($Z = 16$ and $N = 27$) just reflects the degeneracy of the two orbitals, $\nu f_{7/2}$ and $\nu p_{3/2}$, at $Z = 16$ in Fig. 3. On the other hand, the neutron ESPE in the SDPF-U interaction does not show such a strong reduction of the $N = 28$ shell gap from $Z = 20$ to $Z = 16$. At $Z = 16$, the gap still equals about 3.5 MeV, and the inversion between the $7/2^-$ and $3/2^-$ states is ascribed to the combined effect of the gap reduction due to the monopole interactions and the increase of the multipole correlations. The $N = 28$ shell closure is eroded in ^{46}Ar and ^{44}S, after the removal of only two and four protons, respectively. This rapid disappearance of rigidity in the $N = 28$ isotones has been ascribed to a reduction of the neutron shell gap at $N = 28$ combined with that of the proton subshell gap at $Z = 16$, leading to increased probability of quadrupole excitations within the fp and sd shells for neutrons and protons, respectively. In fact, the occurrence of the low-lying isomer at 320.5 keV in ^{43}S has been interpreted in the shell-model framework as resulting from the inversion between $(\nu 7/2^-)^{-1}$ and $(\nu 3/2^-)^{+1}$ configurations [25,27]. We have thus understood that the inversion has the origin of vanishing $N = 28$ magicity at $Z = 16$.

In Fig. 5, the proton ESPE with $Z = 20$ are shown as a function of neutron number. It is seen that the shell gap between the $\pi d_{3/2}$ and $\pi s_{1/2}$ proton orbitals in the double closed-shell nucleus ^{40}Ca ($Z = N = 20$) decreases with increasing neutron number. The $\pi d_{3/2}$ orbit is almost degenerate with the $\pi s_{1/2}$ orbit at $N = 28$ and lies just below the $\pi s_{1/2}$ orbit at $N = 28$. An inversion of the $\pi d_{3/2}$ and $\pi s_{1/2}$ orbits thus occurs above $N = 32$. The effect of adding neutrons to the $f_{7/2}$ orbital is primarily to reduce the proton $s_{1/2}$-$d_{3/2}$ gap. The relevant orbitals, $\pi s_{1/2}$ and $\pi d_{3/2}$, are known to become degenerate at $N = 28$. This degeneracy enhances the quadrupole correlation energy of the configurations with open neutron orbitals. The ESPE from $N = 34$ to $N = 40$ for the $\pi d_{5/2}$ are different from those of the SDPF-U calculations. It would be attributed to the monopole effect between the $\pi d_{5/2}$ and the $\nu f_{5/2}$. Figure 6 shows the energy splitting between the lowest $3/2^+$ and $1/2^+$ states as a function of mass number for the neutron-rich isotopes of phosphorus, chlorine, and potassium. The calculations are in a good agreement with available experimental data [3,24,28] for the

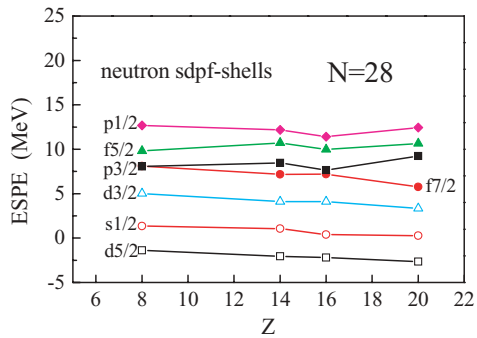

FIG. 3. (Color online) Effective neutron single-particle energies at $N = 28$ from $Z = 8$ to $Z = 20$.

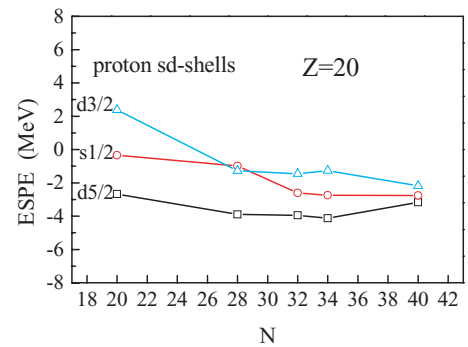

FIG. 5. (Color online) Effective proton single-particle energies at $Z = 20$ from $N = 20$ to $N = 40$.

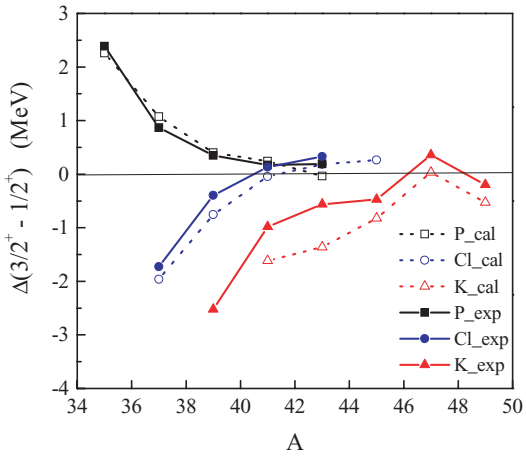

FIG. 6. (Color online) Energy splitting between the lowest $3/2^+$ and $1/2^+$ states in neutron-rich P, Cl, and K isotopes.

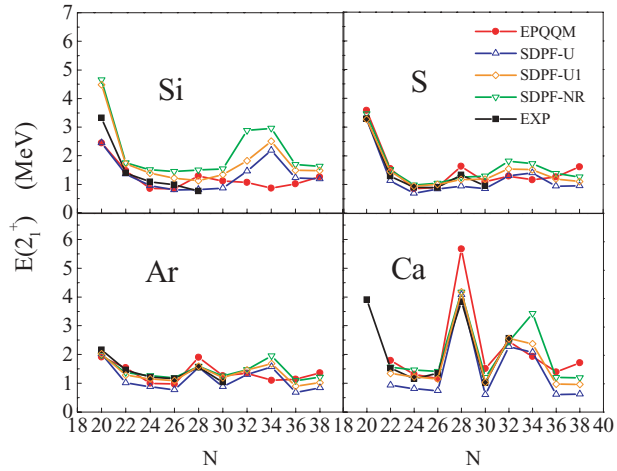

FIG. 7. (Color online) Comparison between experimental and calculated first excited 2^+ energies $E(2_1{}^+)$ with several effective interactions, EPQQM, SDPF-U, SDPF-U1, and SDPF-NR, for Si ($Z = 14$), S ($Z = 16$), Ar ($Z = 18$), and Ca ($Z = 20$) isotopes.

phosphorus and chlorine isotopes but not for the potassium isotopes. The energy splitting between $3/2^+$ and $1/2^+$ for K isotopes in Fig. 6 deviates from the experimental data. This would be related with the disagreement of the first excited 2^+ energies in Fig. 2. The variation trend reflects the reduction of the $\pi d_{3/2}$-$\pi s_{1/2}$ splitting in Fig. 5 as neutron number increases. The inversion of the $\pi d_{3/2}$-$\pi s_{1/2}$ orbits at $N = 28$ corresponds to the observation that the ground state of ^{47}K is actually the $1/2^+$ state, not the expected $3/2^+$ from the hole state $(\pi d_{3/2})^{-1}$. The near degeneracy of $\pi d_{3/2}$ and $\pi s_{1/2}$ is again attributed to the attractive proton-neutron monopole interaction between the $\nu f_{7/2}$ and $\pi d_{3/2}$. The erosion of the $N = 28$ shell gap is enhanced at $Z = 16$ by the degeneracy of the $\pi d_{3/2}$ and $\pi s_{1/2}$ proton orbits. In Fig. 6, we also show the energy splitting between the lowest $3/2^+$ and $1/2^+$ states for the $^{37-45}$Cl nuclei [28].

B. Comparison with other shell-model calculations

A consistent description of collectivity at $N = 28$ for different isotopic chains of the neutron-rich sd-shell nuclei has been a challenge for shell-model calculations. The early calculations with the SDPF-NR interaction described the level scheme and transitions for these isotopic chains. However, it was found that the calculated results deviate from the experimental data. For the silicon isotopes, the calculated energy levels are too high. To improve the agreement, Nowacki and Poves have proposed two effective interactions [12], one (SDPF-U) for $Z \leqslant 14$ and the other (SDPF-U1) for $Z > 14$.

It is interesting to compare the energy levels obtained from the shell-model calculations with different effective interactions (EPQQM, SDPF-U, SDPF-U1, and SDPF-NR). Figure 7 shows the first excited 2^+ energies as a function of neutron number for the Ca, Ar, S, and Si isotopes. The EPQQM calculations agree well with the known experimental data, except for ^{34}Si and ^{44}S. The SDPF-NR calculations also agree with the data for the Ca and Ar isotopes but cannot reproduce those of the Si isotopes. The calculated first excited 2^+ states lie higher than experimental results show. On the other hand, the SDPF-U (SDPF-U1) interaction fails to reproduce the known experimental data for $Z > 14$ ($Z \leqslant 14$). Moreover, considerable differences between the EPQQM and SDPF-NR (and also SDPF-U, SDPF-U1) can be seen around the neutron number $N = 34$, where no experimental data are currently available to discriminate the predictions. We note that none of the interactions can reproduce the first excited 2^+ energy level of ^{34}Si with $N = 20$. This suggests that it would be necessary to include the neutron excitations from the sd shell to the pf shell across the $N = 20$ energy gap. The disappearance of the $N = 20$ magic structure between the sd and pf shells has already been established for the neutron-rich nuclei with $N = 20$ isotones.

C. Level scheme and $B(E2)$ values

In this subsection, we present the theoretical level schemes and electromagnetic $E2$ transition probabilities calculated with the EPQQM interaction and compare the predictions with experimental results. In Fig. 8, we show energy levels for the even-even sulfur isotopes, where for each isotope, the left and right parts of energy levels denote the experimental data [13,24,30] and the calculated energies, respectively. The agreement between the calculation and experiment is fairly good.

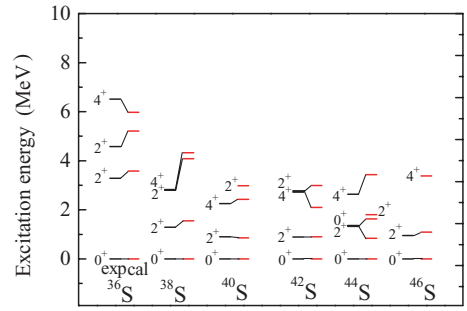

FIG. 8. (Color online) Experimental and calculated energy levels for even-even sulfur isotpes [2,24,29,30]. The left (black) and right (red) bars denote the experimental and calculated energy levels, respectively.

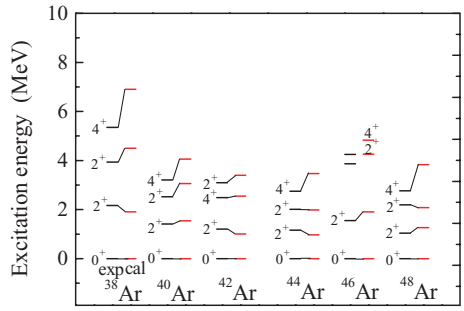

FIG. 9. (Color online) Experimental and calculated energy levels for even-even argon isotopes [24,31,33,34]. The left (black) and right (red) bars denote the experimental and calculated energy levels, respectively.

In particular, the calculated first excited 2^+ energy level for ^{46}S reproduces very well the recently observed data [13]. Very recently, the energy spectrum for ^{44}Ar has been experimentally obtained [31,32]. In ^{40}S, the calculated $E(4_1{}^+)/E(2_1{}^+)$ ratio is about 2.5, which qualitatively suggests a transitional or γ-soft nature for this nucleus. In ^{42}S, the $E(4_1{}^+)/E(2_1{}^+)$ ratio is 3.0, which is quite close to the rigid rotor value. The situation significantly differs in ^{44}S, where both deformed and spherical configurations are predicted to coexist and mix weakly with each other, which is supported by the observation of the low-lying $0_2{}^+$ state at 1.326 MeV [30]. In the shell-model calculation, this state lies below the $2_1{}^+$ state. The presence of a low-lying $0_2{}^+$ state is considered as a signature of a spherical–deformed-shape coexistence, and the present data support the weakening of the $N = 28$ shell gap. Figure 9 shows the energy levels for the even-even argon isotopes. One finds that the calculated energy levels can reproduce the experimental data [24,31]. The first excited 2^+ energy $E(2_1{}^+)$ for Ar isotopes decreases with increasing neutron number from ^{38}Ar to ^{44}Ar, but with a sudden increase for the $N = 28$ isotope. This suggests the persistence of the $N = 28$ gap in Ar nuclei. In Figs. 8 and 9, we note that the rms deviations for the $2_1{}^+$, $2_2{}^+$, and $4_1{}^+$ states are respectively 0.22, 0.71, and 0.92 (in MeV), and the agreement becomes worse with increasing excitation energy. The disagreement may require the further improvement of the EPQQM interaction.

To demonstrate the EPQQM model calculation for odd-mass nuclei in this mass region, we show in Fig. 10 energy levels for some odd-mass S and Ar isotopes. In the comparison,

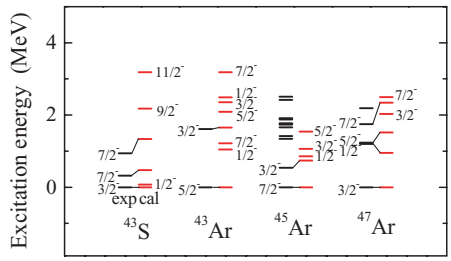

FIG. 10. (Color online) Comparison of calculated energy levels with the recent experimental data for S and Ar nuclei [4,24,25,32,35–37]. The left (black) and right (red) bars denote the experimental and calculated energy levels, respectively.

TABLE I. Calculated $B(E2 : 2^+ \rightarrow 0^+)$ values for the even-even S, Ar, and Si isotopes.

	$B(E2)$ (e^2 fm^4)			
	Exp.	EPQQM	SDPF-U	SDPF-NR
^{36}S	21	22	22	21
^{38}S	47	38	33	34
^{40}S	67	63	58	60
^{42}S	79	72	75	73
^{44}S	63	98	73	73
^{38}Ar	26	35	34	34
^{40}Ar	66	59	49	50
^{42}Ar	86	59	70	72
^{44}Ar	69	47	71	77
^{46}Ar	114	108	105	106
^{36}Si	39	33	34	30
^{38}Si	38	40	39	37
^{40}Si		48	54	46
^{42}Si		64	86	53

the experimental energy levels for ^{43}S and ^{47}Ar are taken from the recent experiments [4,32]. From the calculation, the ground state of ^{43}S is $3/2^-$, not the expected $7/2^-$, suggesting that this nucleus is deformed. The occurrence of a low-lying isomer at 320.5 keV in ^{43}S is interpreted in the shell-model framework as resulting from the inversion between the natural $(\nu f_{7/2})^{-1}$ and the intruder $(\nu p_{3/2})^{+1}$ configurations. Both the low $B(E2; 7/2^- \rightarrow 3/2^-)$ value and the absence of calculated deformed structure built on the $7/2^-$ isomer suggest a coexistence of different shapes in the low-lying structure of the nucleus ^{43}S. In ^{47}Ar, the ground state $3/2^-$ and the excited state $1/2^-$ can be interpreted as a coupling of a $p_{3/2}$ and $p_{1/2}$ neutron to the 0^+ ground state of ^{46}Ar. The $5/2^-$ and $7/2^-$ levels result from the coupling of a $p_{3/2}$ neutron to the $2_1{}^+$ state of ^{46}Ar.

In Table I, we compare $B(E2)$ values between the theoretical calculations and experiments for the S, Ar, and Si isotopes. The experimental $B(E2)$ values are taken from Refs. [1,29,38,39]. In our $B(E2)$ calculations, we take the effective charges e_π for protons and e_ν for neutrons as follows: $e_\pi = 1.35e$ and $e_\nu = 0.35e$ for S isotopes, $e_\pi = 1.50e$ and $e_\nu = 0.50e$ for Ar isotopes, and $e_\pi = 1.15e$ and $e_\nu = 0.15e$ for Si isotopes. On the other hand, in the SDPF-NR and SDPF-U calculations, the effective charges $e_\pi = 1.35e$ and $e_\nu = 0.35e$ suggested in Ref. [12] are used for S and Si isotopes, and the effective charges $e_\pi = 1.50e$ and $e_\nu = 0.50e$ are adopted for Ar isotopes. The $B(E2)$ values were previously calculated and discussed with the SDPF-NR interaction by Retamosa *et al.* [6]. As one can see, our EPQQM calculation is in a good agreement with the experimental $B(E2)$ values for the $^{36-42}$S but is larger than the experimental value for ^{44}S. On the other hand, both the SDPF-U and SDPF-NR calculations also reproduce the data $B(E2)$ except for ^{38,44}S. In Table I, we also compare the calculated $B(E2)$ values with data for the Ar isotopes. The experimental $B(E2)$ values are taken from Refs. [24,29,38,40]. One observes that the experimental $B(E2)$ increases monotonically from ^{38}Ar to the midshell nucleus ^{42}Ar and then decreases toward ^{46}Ar. We note that all the

TABLE II. Calculated spectroscopic quadrupole moments for the first excited 2^+ states in the $N = 28$ isotones.

	Q (e fm^2)			
	Exp.	EPQQM	SDPF-U	SDPF-NR
^{40}Mg		−23	−20	−18
^{42}Si		16	20	15
^{44}S		−3	−16	−15
^{44}Ar	−8	−16	−3.7	−2.5
^{46}Ar		21	21	21
^{48}Ca		5	3	3

theoretical calculations agree fairly well for $^{38-44}$Ar, but for ^{46}Ar the calculated $B(E2)$ values are all too large [34,41]. All the current shell-model calculations with different interactions yield a similar value, which may indicate that this is a robust result. Very recently, however, a new experimental value 114 e^2 fm^4 has been reported [42], and is in a good agreement with all the shell-model predictions. In Table I, this new experimental value is included for comparison. It is apparent from the reduction in excitation energy of the $2_1{}^+$ states and the enhancement in $B(E2)$ that collective features are gradually developed in neutron-rich isotopes between $N = 20$ and $N = 28$. However, a different approach, the self-consistent mean-field calculation by Werner *et al.* [43], yields a much smaller $B(E2)$, in disagreement with the new experimental data. We compare $B(E2)$ values between theoretical calculations and experimental results for the Si isotopes. The agreements with the available data are satisfactory. The $B(E2)$ values increase with increasing neutron number N. The calculated $B(E2)$ values are quite similar for the EPQQM and SDPF-U interactions. For SDPF-NR, however, the predicted values are smaller for the heavier isotopes ^{40,42}Si.

Finally, in Table II, we present calculated spectroscopic quadrupole moments for the $N = 28$ isotones. For all the effective interactions, small, positive Q's are found for ^{48}Ca, indicating a spherical character of this nucleus. For the ^{44}S nucleus, its small $2_1{}^+$ energy, large $B(E2)$ value, and the presence of a second excited $0_2{}^+$ isomer at low excitation suggest a mixed ground-state configuration with spherical and deformed shapes. Recent experiments on the odd mass sulfur isotopes around ^{44}S seem to indicate that ^{44}S is a deformed nucleus with strong shape coexistence, whereas ^{42}S can be considered as a well-deformed system. The enhancement in $B(E2)$ of ^{46}Ar coincides with a shape change from a small prolate deformation in ^{44}Ar to a large deformation in ^{46}Ar. The predicted spectroscopic quadrupole moment $Q_s(2_1^+)$ in ^{44}Ar is somewhat larger than the experimental value, but with a correct sign. In ^{42}Si, the yrast sequence of $0_1{}^+$, $2_1{}^+$, $4_1{}^+$ does not follow the rotational $J(J+1)$ law. However, its quadrupole moments are consistent with a deformed oblate structure. The ground state of ^{40}Mg and that of ^{42}Si are predicted to be prolately and oblately deformed, respectively. All the shell-model calculations consistently indicate a rapid variation in quadrupole moment for the $N = 28$ isotones, suggesting a drastic shape change in this mass region.

IV. CONCLUSIONS

We have investigated the microscopic structure of the neutron-rich sd-shell nuclei using the spherical shell model with a new effective interaction in the sd-pf valence space. The interaction is of the extended pairing plus quadrupole-quadrupole-type forces with inclusion of the monopole interaction. The calculation has reproduced reasonably well the known energy levels for even-even and odd-mass nuclei including the recent data for ^{43}S, ^{46}S, and ^{47}Ar. Special attention has been paid to the $N = 28$ shell-gap erosion. It has been shown that the attractive $T = 0$ monopole interactions $\pi d_{3/2}$-$\nu f_{7/2}$ and $\pi d_{5/2}$-$\nu f_{7/2}$ are very important for the variation of the shell gap at $N = 28$. This shell evolution is considered as the monopole effect of the central and tensor forces in the nucleon-nucleon interaction. The strong attractive monopole interaction $\pi d_{3/2}$-$\nu f_{7/2}$ causes the inversion of the $3/2^+$ and $1/2^+$ states in odd-proton nucleus ^{47}K. However, the inversion is recovered in the neighboring nucleus ^{49}K, which is due to the repulsive monopole interaction $\pi d_{3/2}$-$\nu p_{3/2}$. We have studied the shape change in the neutron-rich $N = 28$ isotones and predicted the drastic shape change when protons are removed from the $Z = 20$ isotone ^{48}Ca, that is, going toward the neutron drip line.

ACKNOWLEDGMENTS

Research at SJTU was supported by a Shanghai Pu-Jiang grant, by the National Natural Science Foundation of China under Contract No. 10875077, and by the Chinese Major State Basic Research Development Program through Grant No. 2007CB815005.

[1] H. Scheit *et al.*, Phys. Rev. Lett. **77**, 3967 (1996).
[2] D. Sohler *et al.*, Phys. Rev. C **66**, 054302 (2002).
[3] B. Bastin *et al.*, Phys. Rev. Lett. **99**, 022503 (2007).
[4] L. Gaudefroy *et al.*, Phys. Rev. Lett. **102**, 092501 (2009).
[5] O. Sorlin *et al.*, Eur. Phys. J. A **22**, 173 (2004).
[6] J. Retamosa, E. Caurier, F. Nowacki, and A. Poves, Phys. Rev. C **55**, 1266 (1997).
[7] S. Nummela *et al.*, Phys. Rev. C **63**, 044316 (2001).
[8] E. Caurier, F. Nowacki, A. Poves, and J. Retamosa, Phys. Rev. C **58**, 2033 (1998).
[9] E. Caurier, F. Nowacki, and A. Poves, Eur. Phys. J. A **15**, 145 (2002).
[10] E. Caurier, G. Martinez-Pinedo, F. Nowacki, A. Poves, and A. P. Zuker, Rev. Mod. Phys. **77**, 427 (2005).
[11] J. Fridmann *et al.*, Nature **435**, 922 (2005).
[12] F. Nowacki and A. Poves, Phys. Rev. C **79**, 014310 (2009).
[13] A. Gade *et al.*, Phys. Rev. Lett. **102**, 182502 (2009).
[14] M. Dufour and A. P. Zuker, Phys. Rev. C **54**, 1641 (1996).
[15] M. Hasegawa, K. Kaneko, and S. Tazaki, Nucl. Phys. A **688**, 765 (2001).
[16] K. Kaneko, M. Hasegawa, and T. Mizusaki, Phys. Rev. C **66**, 051306(R) (2002).

[17] K. Kaneko, Y. Sun, M. Hasegawa, and T. Mizusaki, Phys. Rev. C **78**, 064312 (2008).
[18] T. Otsuka, R. Fujimoto, Y. Utsuno, B. A. Brown, M. Honma, and T. Mizusaki, Phys. Rev. Lett. **87**, 082502 (2001).
[19] T. Otsuka, T. Suzuki, R. Fujimoto, H. Grawe, and Y. Akaishi, Phys. Rev. Lett. **95**, 232502 (2005).
[20] N. A. Smirnova, B. Bally, K. Hyde, F. Nowacki, and K. Sieya, Phys. Lett. B **686**, 109 (2010).
[21] T. Otsuka, T. Suzuki, M. Honma, Y. Utsuno, N. Tsunoda, K. Tsukiyama, and M. Hjorth-Jensen, Phys. Rev. Lett. **104**, 012501 (2010).
[22] T. Otsuka, T. Suzuki, and Y. Utsuno, Nucl. Phys. A **805**, 127c (2008).
[23] E. Caurier, code ANTOINE, Strasbourg, 1989 (unpublished).
[24] National Nuclear Data Center, Brookhaven National Laboratory, [http://www.nndc.bnl.gov/ensdf/].
[25] L. Gaudefroy *et al.*, Phys. Rev. C **78**, 034307 (2008).
[26] L. A. Riley *et al.*, Phys. Rev. C **78**, 011303(R) (2008).
[27] F. Sarazin *et al.*, Phys. Rev. Lett. **84**, 5062 (2000).
[28] L. A. Riley *et al.*, Phys. Rev. C **79**, 051303(R) (2009).
[29] A. E. Stuchbery *et al.*, Phys. Rev. C **74**, 054307 (2006).
[30] C. Force *et al.*, Phys. Rev. Lett. **105**, 102501 (2010).
[31] M. Zielinska *et al.*, Phys. Rev. C **80**, 014317 (2009).
[32] S. Bhattacharyya *et al.*, Phys. Rev. Lett. **101**, 032501 (2008).
[33] A. Gade *et al.*, Phys. Rev. C **68**, 014302 (2003).
[34] L. A. Riley *et al.*, Phys. Rev. C **72**, 024311 (2005).
[35] T. Baumann *et al.*, Nature (London) **449**, 1022 (2007).
[36] L. Gaudefroy *et al.*, Phys. Rev. Lett. **97**, 092501 (2006).
[37] A. Gade *et al.*, Phys. Rev. C **71**, 051301 (2005).
[38] S. Raman *et al.*, At. Data Nucl. Data Tables **78**, 1 (2001).
[39] T. Glasmacher *et al.*, Annu. Rev. Nucl. Part. Sci. **48**, 1 (1998).
[40] K.-H. Speidel *et al.*, Phys. Rev. C **78**, 017304 (2008).
[41] S. J. Q. Robinson, Y. Y. Sharon, and L. Zamick, Phys. Rev. C **79**, 054322 (2009).
[42] D. Mengoni *et al.*, Phys. Rev. C **82**, 024308 (2010).
[43] T. R. Werner *et al.*, Phys. Lett. B **335**, 259 (1994); Nucl. Phys. A **597**, 327 (1996).